INTERNATIONAL JOURNAL OF GREEN ENERGY
2024, VOL. 21, NO. 10, 2218–2227
https://doi.org/10.1080/15435075.2023.2297781

Green heterogeneous catalysts derived from fermented kola nut pod husk for sustainable biodiesel production

Asuquo Jackson Asuquo[a], Xiaolei Zhang[a], Leteng Lin[b], and Jun Li[a]

[a]Department of Chemical & Process Engineering, University of Strathclyde, Glasgow, UK; [b]Department of Built Environment and Energy Technology, Linnaeus University, Växjö, Sweden

ABSTRACT

The use of green heterogeneous catalysts that are obtained from waste agricultural biomass can make the production of biodiesel more economical. In this research, three solid base heterogeneous catalysts (Catalyst A, B, and C) were synthesized from kola nut pod husks, and the synergistic effects of the elemental composition on catalytic activities for biodiesel production were studied. The results revealed a high surface area of Catalysts A, B, and C at 419.90 m^2/g, 430.54 m^2/g, and 432.57 m^2/g, respectively. Their corresponding pore diameters are 3.53 nm, 3.48 nm, and 3.32 nm, showing that the catalysts are mesoporous in nature. The X-ray Fluorescence (XRF) results revealed the presence of a variety of alkaline earth metals and their corresponding metal oxides in substantial amounts. Catalyst A was produced with the highest concentration of calcium at 40.84 wt.% and calcium oxide at 68.02 mole%. The substantial concentration of other elements, such as potassium, magnesium, and aluminum, and their corresponding metal oxides are the proof of high catalytic activity of the produced green catalysts. The high CaO contents of all three produced catalysts and their high surface areas indicate their strong potential for good catalytic activities applied to the synthesis of biodiesel.

ARTICLE HISTORY
Received 25 October 2023
Accepted 16 December 2023

KEYWORDS
Biodiesel production; green catalyst; synthesis; characterization; sustainability

1. Introduction

The continuous and extensive use of fossil fuels have led to growing worries about the adverse effects on the environment, which bothers mainly on greenhouse gas emissions (Kamble et al. 2022). According to the Stanford Earth Magazine, the total CO_2 emissions in 2020 was approximately 39 $GtCO_2$ (Stanford University 2020). In order to reduce this emissions level, EU countries and others have agreed under the Paris Agreement a road map to achieving net-zero carbon emissions by 2050 (European Climate Foundation 2023). One of the viable options of achieving this is by using an alternative source of fuel such as biodiesel (Dias et al., 2016). Biodiesel can be obtained from plant and animal sources such as Jatropha, Soybean, palm oil, rapeseed oil, and *Carica papaya* seed oils, among others (Tan et al. 2023). These alternative sources of fuel have been reported to significantly reduce hydrocarbon, CO, and soot emissions (Tan et al. 2023). Therefore, the use of biodiesel to replace conventional transport fuels that derived from fossils could contribute to achieving this feat. Biodiesel has numerous advantages; it is renewable and so with lower carbon emissions, environmentally friendly, and miscible with petro-diesel. However, the high cost of the feedstock restricts a wider utilization of biodiesel, around 80–85% cost of producing biodiesel is related to the feedstock cost (Betiku et al. 2019). A promising way to reduce this cost is by using low economic feedstock from biomass waste.

The utilization of homogenous catalysts in biodiesel synthesis have posed a lot of issues such as inability to recover used catalysts, the requirement of expensive catalyst purification and removal steps, corrosion of equipment, production of soap and glycerol as by-products, and enormous production of wastewater, thereby making the entire process environmentally harmful and the purification steps very expensive (Asogwa, Anikwe, and Mokwunye 2006; Betiku, Akintunde, and Ojumu 2016). To overcome the above setbacks from the use of homogenous catalysts, the utilization of the renewable heterogeneous catalysts for fatty Acid Methyl Esters (FAME) production have been considered more advantageous compared to traditional homogenous catalysts. The green catalysts are neither consumed nor dissolved in the transesterification reaction for biodiesel production, thereby making the reaction more effective and cheaper (Asogwa, Anikwe, and Mokwunye 2006; Betiku, Akintunde, and Ojumu 2016). Notwithstanding, it has been reported that some heterogeneous catalyst has the tendency of leaching into the reaction mixture during biodiesel production; hence, the need for solid support to ensure that the catalyst is immobilized at the surface (Xie et al, 2018; Xie et al. 2020)

Kola nut pod husk is a waste biomass derived from kola trees, which are widespread in West African countries. There are well over 40 different species of kola nuts, and of all of these, the Cola Acuminata and Cola Nitida are of great social and economic values in African countries, e.g., Nigeria (Betiku et al. 2019). In 2020, the world production of kola nut was 304,950 tonnes out of which Nigeria produced 166,895 tonnes,

CONTACT Jun Li jun.li@strath.ac.uk Department of Chemical & Process Engineering, University of Strathclyde, James Weir Building, 75 Montrose Street, Glasgow G1 1XJ, UK

which accounted for 54.7% of the production thereby making Nigeria as one of the world's largest kola nut producers (UN, 'World kola nut production' 2022). With the large availability of this resource, if it is disposed directly into the surrounding environment, it could pose an environmental hazard triggering release of harmful greenhouse gases such as methane (Betiku et al. 2019). The development of a biocatalyst from kola nut pod husk is receiving growing interests and suggests that it could be developed as a base catalyst for biodiesel production (Betiku et al. 2019). Recent studies have focused on the development of green heterogeneous catalysts and their application for FAME synthesis due to the rich inherent minerals in biomass and agro-waste materials that are suitable for green heterogeneous catalysts production, as summarized in Table 1. This is because the solid base catalysts used are not consumed during the reaction and so can easily be separated from the biodiesel product. These solid base catalysts are active at the boiling point of methanol (MeOH) during transesterification process (Adepoju et al. 2018; Uddin et al. 2013).

To buttress this claim, researchers have investigated the catalytic activities of various heterogeneous catalysts. Olugbenga et al (Olugbenga, Mohammed, and Ajakaye 2013) have reported the use of cocoa pod husk catalyst for the conversion of waste vegetable oil (WVO) using 5 wt.% amount of catalyst, MeOH:WVO molar ratio of 50:1 at a temperature of 60°C for 300 min, resulting in a biodiesel yield of 94 wt.%. Musa acuminata peduncle ash was used for the transesterification Ceiba Pentandra oil (CPO) to 98.5 wt. %, which was achieved under the transesterification conditions of 1.98 wt.% catalyst loading, MeOH: CPO molar ratio of 9.20:1 at 60 oC for 60 min (Balajii and Niju 2019). Vadery et al (Vadery et al. 2014) also reported the use of coconut husk catalyst for the conversion via transesterification of Jatropha oil (JO) using 7 wt.% of catalyst amounts, MeOH: JO molar ratio of 12:1, at a temperature of 45°C for 30 min to synthesize 99.86 wt.% biodiesel. Kola nut pod husk catalyst was employed by Betiku et al (Betiku et al. 2019). for the conversion of Kariya oil (KO) to biodiesel yield of 98.67 wt.% under catalyst loading of 3 wt.%, MeOH: KO molar ratio of 6:1 at 65°C for 75 min. Osakwe et al (Osakwe et al. 2018) also transesterified yellow oleander oil (YOO) using kola nut pod husk catalyst to produce 84.5 wt. % biodiesel under MeoH:YOO molar ration of 6:1, catalyst amount of 1.5% at a temperature of 60°C for 90 min. Esther et al (Olatundun, Borokini, and Betiku 2020) have combined two agro-wastes of cocoa pod husk and plantain peel heterogeneous catalyst for the transesterification of hone seed oil (HSO) to obtain a maximum biodiesel yield of 98.98 wt.% with catalyst loading amount of 4.5 wt.%, reaction temperature of 65°C, time of 2.5 h and MeOH:HO blend molar ratio of 15:1. Most recently, Falowo et al (Falowo et al. 2020) produced a catalyst from three agro-wastes of equal mixture of cocoa pod husk, plantain peel and kola nut pod husk ashes for the transesterification of a blend of hone, rubber and neem oils (HRNO) in a volumetric ratio of 20:20:60, to obtain a maximum biodiesel yield of 98.45 wt.% from MeOH:HRNO blend molar ratio of 12:1, catalyst concentration of 1.158 wt.% and a reaction time of 60 min.

Despite the array of reports available in the literature on the synthesis of green catalysts for biodiesel production, there are still challenges in terms of conversion efficiency, catalyst recovery and reusability, availability and affordability among others. These issues have necessitated the search for novel catalysts to meet the growing demand for green fuel. To the best of our knowledge, reports on fermentation of kolanut pod husk for application as a heterogeneous catalyst for synthesis of biodiesel is rather rare. In 2020, Adepoju et al (Adepoju et al. 2020). reported a boost of calcium and potassium mineral content after fermentation of kola nut pod husk for the transesterification of Butyrospermum parkii (Shea butter) oil (BPO) to biodiesel. However, the surface area of the catalyst was rather low as 1.2 m^2/g (Bharti, Singh, and Dey 2019), a high surface area of catalyst would likely have more active sites required for good conversion efficiency during biodiesel production. It is thus important to assess the conditions required to improve the surface area and other catalytic properties required for biodiesel production. This research focuses on preparation of catalyst from kola nut pod husk with

Table 1. Summary of waste agro-based catalysts and vegetable oil feedstock used in biodiesel synthesis via transesterification.

	Calcination conditions			Transesterification conditions				FAME Yield	
Catalyst	Heat (°C)	Time (h)	Oil feedstock	MeOH:Oil ratio	Catalyst (Wt. %)	Temp (°C)	Time (min)	(Wt. %)	Refs.
Musa acuminata (Red banana) peduncle	700	4	*Ceiba pentandra oil*	11.46	2.68	65	106	98.73	(Balajii and Niju 2019)
Carica papaya peels	700	4	Used vegetable oil	12:1	3.5	65	60	97.5	(Etim, Eloka-Eboka, and Musonge 2021)
Kola nut pod husk	500	4	*Kariya* oil	6:1	3	65	75	98.67	(Betiku et al. 2019)
Kola nut husk	600	3	Yellow oleander	6:1	1.5	60	90	84.5	(Osakwe et al. 2018)
Cocoa pod husk, plantain peel, kola nut pod husk	500	4	Honne-rubber-neem oil blend	12:1	1.16	150 W	6	98.45	(Falowo et al. 2020)
Palm kennel shell bio- char	800	2	Sunflower oil	9:1	3	65	240	99.8[a]	(Kostić et al. 2016)
Ostrich-egg shell	1000	4	Used cooking oil	12:1	1.5	65	120	96[b]	(Tan et al. 2015)
Coconut husk	350	1	Jatropha oil	12:1	7	45	45	99[a]	[21]

[a]Methyl ester content (wt. %); [b] Production yield (wt. %).

emphasis on the treatment conditions to optimize the surface area, porosity, functionality, and crystallinity of the catalysts. This will help to assess the suitability of the catalyst for biodiesel production.

2. Materials and methods

2.1. Materials

Kola nut pod husks were collected from Mkpat Enin village in Southern Nigeria. The fresh kola pods were washed with distilled water to remove impurities. 5 kg of the clean pods were placed in a bucket, soaked, and completely submerged in distilled water. Fermentation of the pods was carried out for 10 days as previously reported by Adepoju *et al* (Adepoju et al. 2020). The fermented product was rinsed thoroughly in distilled water and oven dried at 85°C to a constant weight. The dried pods were ground using a blender and sieved to particle size of 0.5 mm. The sieved powder was divided into three equal portions of 10 g each before pre-treatment with methanol and calcination (Adepoju et al. 2018; Betiku et al. 2019).

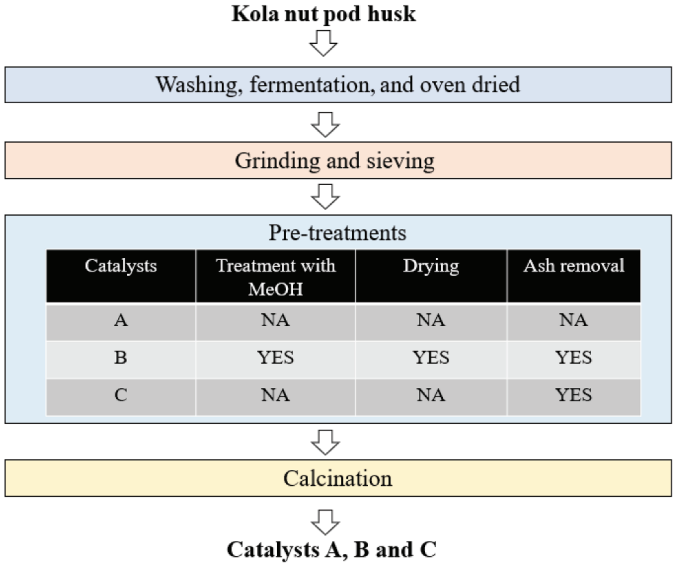

Catalysts	Treatment with MeOH	Drying	Ash removal
A	NA	NA	NA
B	YES	YES	YES
C	NA	NA	YES

Figure 1a. Catalysts preparation process.

2.2. Kola nut pod husk preparation for catalysts production

Figure 1 shows the process for the preparation of three catalysts studied in this work. Catalyst A was not pre-treated with Methanol (MeOH) and so no drying was required; the ash content after calcination was not removed. Catalyst B was pre-treated with MeOH, and it was therefore dried before calcination and after calcination, and the ash content was shaken off. Catalyst C was not pre-treated with MeOH and therefore drying was not required and the ash content was shaken off. Catalyst calcination was done to see the improvement on the surface areas as well as the elemental compositions of the three produced catalysts. The catalysts were calcined differently using Thermoconcept KLS 10/12/WS furnace at the temperature of 700°C for 4 hours. This temperature was chosen because an initial evaluation of the effect of calcination temperature on the surface properties of the catalyst derived from kolanut pods has revealed an optimum temperature of 700°C which gave a high surface area and other physicochemical properties required for the target application (16). The biocatalysts after calcination were placed in airtight glass vials and stored in a desiccator for further processing. The three calcined catalysts can be directly used as renewable heterogeneous catalysts without additional treatment (Betiku et al. 2019).

2.3. Catalysts characterization

To study the surface morphologies of the Fermented Uncalcined Kola Nut Pod Husk (FKPH) raw material and the three Fermented and Calcined Kola Nut Pod Husk catalysts (namely Catalysts A, B and C), a high-resolution scanning electron microscope (SEM)-PhenomProX fitted with energy dispersive X-ray (EDX) detector were used. To ascertain the elemental as well as the metal oxide compositions of the FKPH raw material and the produced catalysts, a Xenemetrix Genius IF X-Ray Fluorescence analyzer was used. To determine the crystallinity of the catalysts, X-Ray Diffractometer analysis was done by using Rikagu MiniFlex 600 analyzer. To ascertain the effectiveness of the calcination process on the surface areas of the synthesized catalysts, a BET Micrometrics ASAP 2420 Surface Area and Porosity Analyser was used. The BET surface area and the BJH desorption (pore size and pore volume)

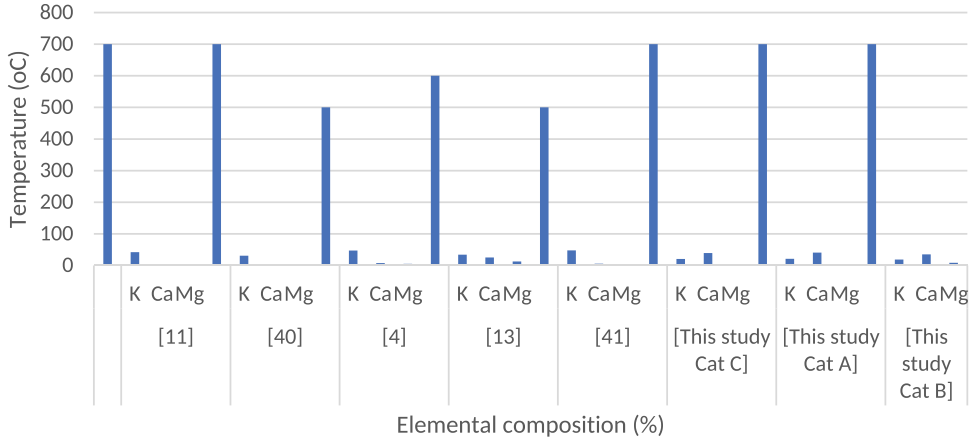

Figure 1b. A comparison of the elemental composition of the synthesized catalyst with some reports in the literature.

methods were employed. ABB Spectra FTIR Spectrophotometer MB 3000 was used to obtain the infrared (IR) spectra of the bio-samples to assess the functional groups inherent in the samples.

3. Results and discussion

The results obtained from the characterization of fermented and calcined Kola Nut Pod Husk catalysts using X-Ray Fluorescence (XRF), Scanning Electron Microscopy- Energy Dispersive X-Ray (SEM-EDX), X-Ray Diffraction (XRD), BET analysis, and Fourier Transform Infra-Red Spectroscopy (FT-IR) are discussed, with aims of determining the yield and properties of the synthesized catalysts to ascertain their suitability for production of biodiesel.

3.1. Catalyst yield

After being treated under various conditions, Fermented Kola Nut Pod Husk samples were calcined to produce catalysts A, B, and C. The mass of each sample was weighted before and after the calcination. The yield of each catalyst was obtained using Equation 1, and the result is presented in Table 2.

$$Catalyst\ yield(\%) = \frac{Mass\ of\ catalyst\ after\ calcination(m_2)}{Mass\ of\ catlyst\ before\ calcination(m_1)} \times 100$$

3.2. Metals and metallic oxide composition

Figure 2 shows that the catalysts are rich in elements such as potassium, calcium, magnesium, and oxygen, while the elements that were present in minor amounts include silicon, aluminum, and sulfur. Comparing the elemental compositions of the FKPH raw sample and catalyst A, B and C, it can be observed that there has been a considerable boost in the elemental compositions of the produced catalysts A, B and C compared to the feedstock. At 700°C, Catalyst A sample was observed to give the highest mole fraction of calcium (40.84 mole %), followed by Catalyst C (39.39 mole %) and Catalyst B sample (35.18 mole %), respectively. The same trend was also observed for potassium, the mole fraction of K was highest in Catalyst A sample with 20.95 mole%, followed by Catalyst C sample of 20.60 mole% and Catalyst B sample of 18.70 mole%.

Magnesium was highest in Catalyst B, and this could be attributed to the pre-treatment with MeOH; Catalyst C sample gave a mole fraction of 2.81 mole%; Mg was not detected in Catalyst A sample. It is worth noting that there is magnesium and magnesium oxides in both catalysts B and C implies the possibility of magnesium deposits during sieving. The calcium composition for Catalysts A, B and C are higher than that of the feedstock sample. A slight increase in the amounts of the elements present in the Catalysts as compared to the FKPH sample is an indication of the effectiveness of the fermentation, calcination, and MeOH pre-treatment processes, which has effectively extracted and boosted the minerals present in the FKPH sample through the breakdown of lignin-carbohydrate matrix (Balajii and Niju 2019).

The results of the key metallic composition obtained from this current study was compared with available reports in the literature, as presented in Table 3. The findings of this study revealed that single base metal oxides such as Cao, MgO, and K_2O, which are the key constituents of solid base heterogeneous catalysts gave equal yield at low temperatures and within a short time (Lee et al. 2014; Maroa and Inambao 2021; Mierczynski et al. 2015). According to Baskar et al (Baskar and Soumiya 2016), CaO catalysts are commonly used in the production of biodiesel due to their low cost and high reactivity under low FFA (<1%).

Table 2. The yields of catalysts.

Catalyst	Mass of the sample before calcination (m_1, g)	Mass of catalysts after calcination (m_2, g)	Yield ($\frac{m_2}{m_1}$, %)
A	10	0.9558	9.56
B	10	0.5825	5.83
C	10	0.6847	6.85

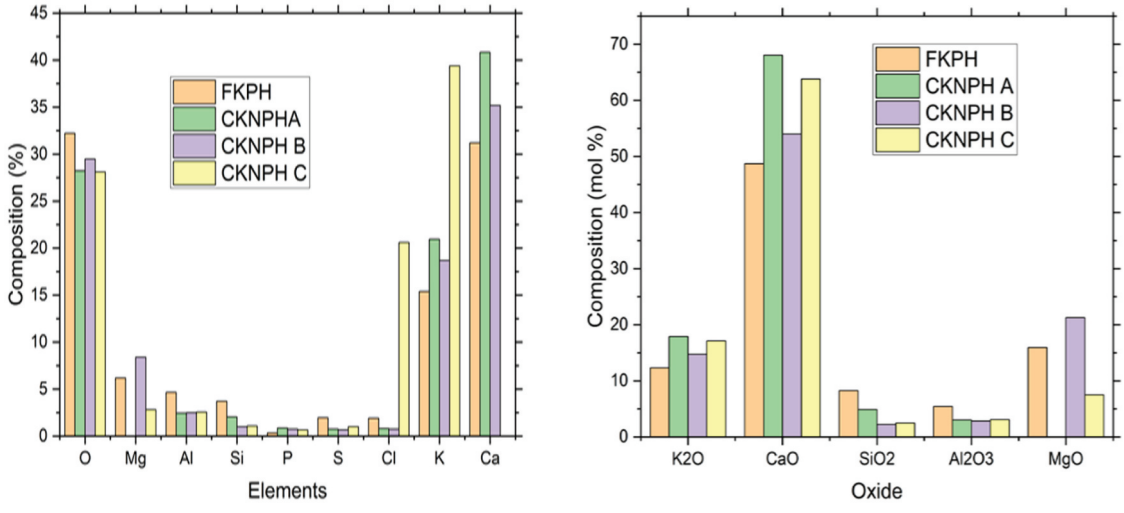

Figure 2. Metal and metallic oxide composition catalyst A, B and C catalysts in comparison to FKPH raw material.

Table 3. Effect of biomass pre-treatment on elemental composition of various catalysts.

Bio-Catalysts	Treatment methods	Calcination conditions		Resulting metallic Contents (%)		Remarks
		Temp. (°C)	Time (h)			
Musa acuminata (Red banana) peduncle	Oven dried at 650°C for 4 days	700	4	K Ca	42.23 1.70	(Balajii and Niju 2019)
Carica papaya peels	Sun-dried for 2 weeks	700	4	K Cl P S	30.74 10.30 3.64 4.31	(Etim, Eloka-Eboka, and Musonge 2020)
Kola nut pod husk	Burnt to ash in open air	500	4	K Ca Mg	47.14 7.59 5.32	(Betiku et al. 2019)
Kola nut husk	Sun drying for 30 days	600	3	K Ca Mg	33.91 25.38 12.40	(Osakwe et al. 2018)
Cocoa pod husk, plantain peel, kola nut pod husk	Open combustion in air	500	4	K Ca Mg	47.60 5.56 4.21	(Falowo and Betiku 2022)
Calcined kola nut pod husk A	Fermentation	700	4	K Ca Al Mg	20.95 40.84 2.44 0.00	This study
Calcined kola nut pod husk B	Fermentation, pre-treatment with MeOH	700	4	K Ca Al Mg	18.70 35.18 2.48 8.40	This study
Calcined kola nut pod husk C	Fermentation, ash removal after calcination	700	4	K Ca Al Mg	20.60 39.39 2.55 2.81	This study

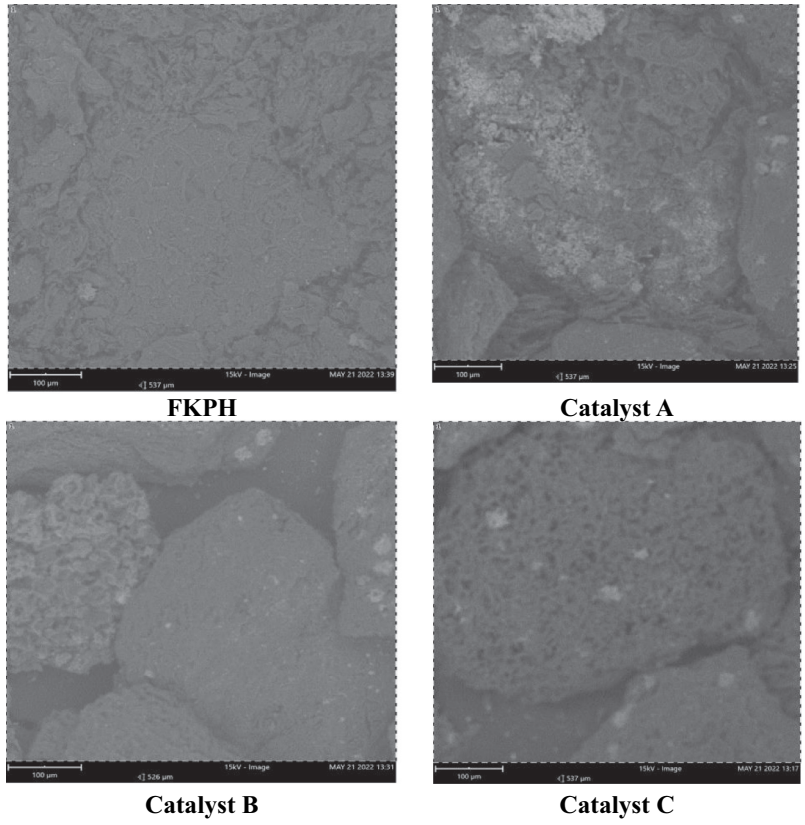

Figure 3. Micrographic images of Catalysts A, B and C in comparison to the raw sample FKPH.

3.3. Morphological studies

The micro-changes in the surface morphological features of the fermented and calcined kola nut pod husk catalysts were assessed using SEM-EDX analysis. The physical impact of the calcination heat process on the produced bio-samples are shown in Figure 3. As observed, raw FKPH sample shows an irregular cracks and porous morphology caused by the manual size reduction process in the fermented sample. The highly disorganized FKPH morphology shows absence of pores and cracks on its heterogeneous surface (Balajii and Niju 2019). The rough surface of the FKPH sample can be attributed to the carbohydrate-lignin matrix during calcination at 700°C for 4 hours. The figure also shows the smooth textured ash catalyst samples produced. The SEM images show the spongy and porous nature of the particles, which are characterized by increased particles agglomeration, which has led to smaller aggregates of particles with high fibrous and mesoporous nature.

The calcined biomass ash used for biodiesel production have been shown to possess spongy and little mineral aggregates agglomeration caused by sintering of metal oxides (Betiku et al. 2019). The calcined ashes can be employed directly as a solid heterogeneous base catalyst for Fatty Acid Methyl Esters (FAME) production (Balajii and Niju 2019). Figure 3 also shows that the produced biocatalysts A, B, and C display relatively ordered, flat, and smooth surface having a lot of pores and perforations. This increased porosity greatly boosts the biodiesel conversion due to their increased surface area as shown in the BET surface area results.

The micro-change in the morphology of the calcined catalysts is known as an indication that the MeOH pre-treatment and calcination temperature have greatly altered the morphology of the raw FKPH feedstock. The Catalysts A, B and C SEM micrographs in Figure 3 indicates the evolution of pores as a function of thermal cracking of the organic compounds and effective treatment (Kamble et al. 2022). When compared with XRF result, it was seen that K, Ca are the major elements. Mg, Mn, Zn, Cu, N, Cr, Fe, and Ni were also found in minute quantities in sample Catalyst B. It was also observed that S and Cl are non-existent in catalyst samples. The most clear and bright particles are majorly comprised of inorganic matter, particularly alkali and alkaline earth metals, as well as Fe. The SEM micrographs also shows the giving off larger number of pores in small areas or points during thermal cracking influenced by mineral oxides such as CaO, K_2O, etc. Minerals and their oxides play catalytic role at the micro-level (Kamble et al. 2022).

Table 4. BET surface area and pore properties of the synthesized catalysts.

Catalyst	Surface Area (m^2/g)	Pore Volume (cm^3/g)	Pore diameter (nm)
A	420	0.25	3.53
B	430.5	0.26	3.48
C	432.6	0.25	3.32

3.4. BET surface area

Table 4 shows a summary of the BET results obtained. The surface areas of Catalysts A, B and C were found to be 419.9 m^2/g, 430.5 m^2/g, and 432.6 m^2/g, respectively. It is observed that both the BET surface areas and BJH desorption summary (pore volume and pore size) show an increase in the values, and this indicates the efficiency of the calcination process and pre-treatment with methanol on the calcined kola nut pod husk catalysts. From Table 4, it is observed that Catalyst A gave the lowest BET surface area, and this could be attributed to the blocking of the pores due to esters, glycerol, and biomass ash content (Balajii and Niju 2019). Catalyst B gave an improved surface area, and this is due to the pre-treatment with methanol and removal of ash content by sieving. Catalyst C sample gave the highest surface area, and this could be caused by the removal of ash content from the catalyst surface formed during calcination process. The effects of calcination temperature, performed size reduction, and sieving process have been reported to aid the high surface area of produced biomass solid catalysts (Adepoju et al. 2018, 2018, 2018, 2020; Balajii and Niju 2019). Table 5 shows a summary of the BET results reported on different biomass catalysts; it shows that the produced Catalysts A, B, and C have significantly higher surface area in comparison to biomass-derived ash-contained solid catalysts.

The BET adsorption-desorption isotherm plot of the catalysts as well as the pore size distribution are shown in Figure 4. All three catalyst samples show a type IV isotherm with type H3 hysteresis loop according to IUPAC classification. This indicates that the material has a higher mesoporosity with more of physical adsorption, suggesting the initial adsorption interactions are followed by pore condensation where there is a phase change from gaseous to liquid state within the pores at a pressure that is less than the saturation pressure of the bulk liquid (Thommes et al. 2015). This is confirmed by the pore size distribution plot in Figure 4, which indicates a broad spectrum covering both microporosity (<2 nm) to macroposority (>50 nm) with more pores around the mesoporous range (2 nm-50 nm). This attribute is characteristic of hierarchical architectures which is highly desirable as a heterogeneous catalyst.

3.5. XRD analysis

The identification of minerals and phases present in the fermented and calcined samples was carried out using XRD analysis. The XRD technique was used to determine the crystallinity of the biomass ash samples. The XRD diffractograms for the fermented and calcined catalysts are shown in Figure 5. The intensity of the peak patterns for Catalysts A, B, and C increased because of the calcination temperature of 700°C and methanol pre-treatment. This heating temperature has increased the crystallinity of the calcined catalysts as observed, similar results as been obtained by other report (Etim, Eloka-Eboka, and Musonge 2021). The results of EDX, FTIR and XRD all support the view that K, Mg, and Ca are the major metallic elements present in Catalysts A, B, and C and have showed to have strong catalytic characteristics in biodiesel production (Betiku et al. 2019). By comparing the XRD patterns of FKPH raw material and Catalysts A, B and C, most of the peaks identified were

Table 5. Summary of BET results reported on different biomass catalysts.

	Surface area (m^2/ g)	Pore volume (cc/g)	Pore diameter or radius (nm)	Biodiesel yield (%)	Refs
Mesua ferrea Linn seed derived char	23.419	7.5206	-	-	(Bora et al. 2018)
Mesua ferrea Linn seed derived activated carbon	333.833	115.63	-	-	(Bora et al. 2018)
Mesua ferrea Linn seed derived sulfonated carbon	150.326	55.32	-	-	(Bora et al. 2018)
Date pits powder	432	0.22[C]	6.62[D]	-	(Abu-Jrai et al. 2017)
Date pits derived carbon catalyst	211	0.14[C]	5.98[D]	91.6	(Abu-Jrai et al. 2017)
Flamboyant pods derived carbon catalyst	820	0.3534[C]	-	89.81	(Dhawane, Kumar, and Halder 2016)
Char	354	0.34C	3.8[R]	-	(Ahmad et al. 2018)
Wood char catalyst	337	0.24[C]	2.7[R]	96	(Ahmad et al. 2018)
Pomelo peel bio char catalyst	6.7	24.4[MM]	-	98	(Zhao et al. 2018)
Wood ash	9.38	-	25[P]	40.2	(Sharma et al. 2012)
Calcined wood ash catalyst	3.72	-	26[P]	98.7	(Sharma et al. 2012)
Activated wood ash catalyst	0.65	-	53[P]	99	(Sharma et al. 2012)
Lemna perpusilla Torrey ash	9.622	2.170×10^{-8} [M]	4.512×10^{-9} [R, M]	89.43	(Chouhan and Sarma 2013)
Musa "Gross Michel" peel ash	4.442	0.020[C]	17.864[D]	98.5	(Betiku, Akintunde, and Ojumu 2016)
Tucuma peel ash	1.0	-	-	97.3	(Mendonça et al. 2019)
Musa balbisiana Colla peel	10.176	0.065	1.60[R]	-	(Gohain, Devi, and Deka 2017)
Musa balbisiana Colla peel ash	14.036	0.074	2.603[R]	100	(Gohain, Devi, and Deka 2017)
Uncalcined red banana Peduncle	24.466	0.083	11.754	-	(Balajii and Niju 2019)
Calcined red banana Peduncle	45.992	0.145	9.770[D]	98.73 ± 0.50	(Balajii and Niju 2019)

[a]Pore radius; [R,M]Pore radius expressed in m; [D]Pore Diameter; [S] Particle Size expressed in μm; [C]Pore Volume expressed in cm^3/g; [M]Pore Volume expressed in m^3/g, [MM]Pore Volume expressed in mm^3/g.

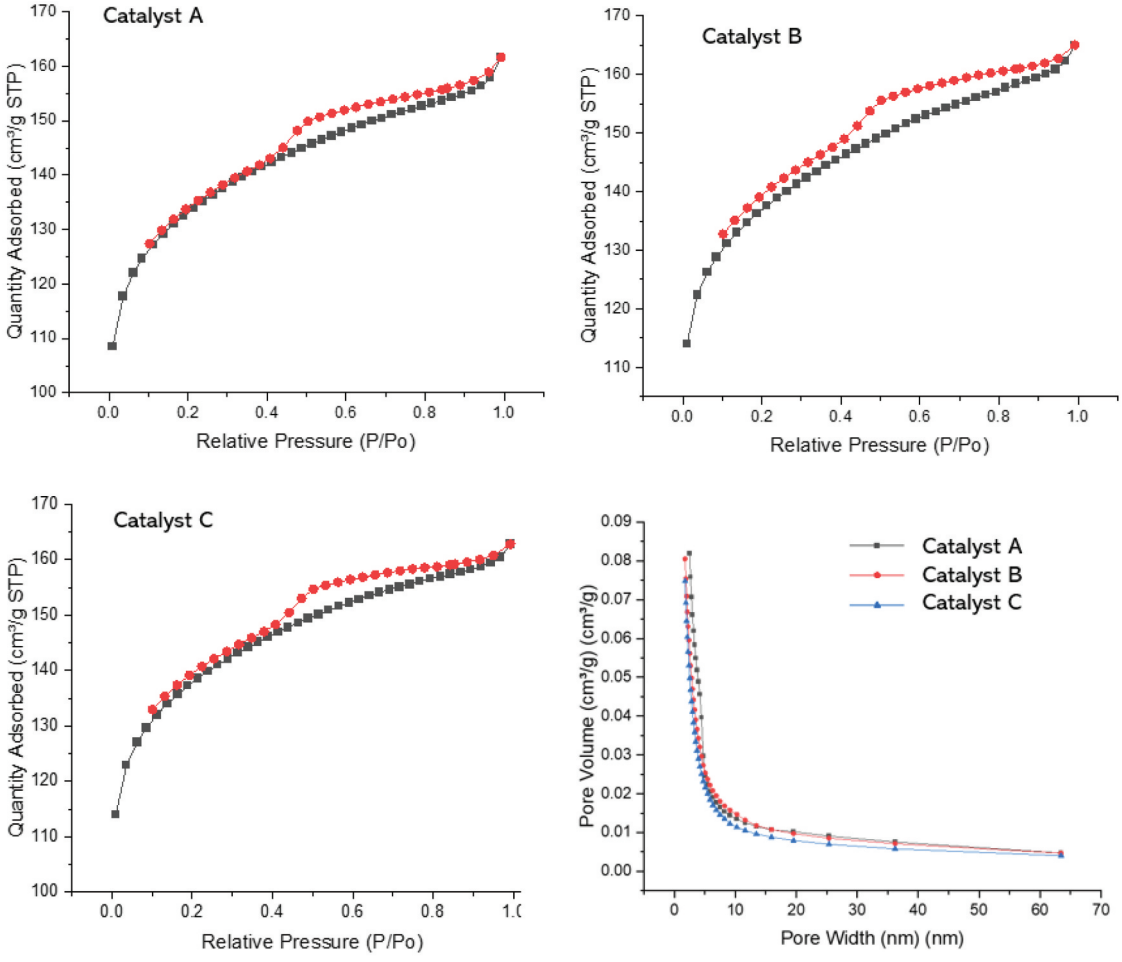

Figure 4. BET adsorption/desorption isotherm plot of catalyst A, B and C, and their pore size distribution.

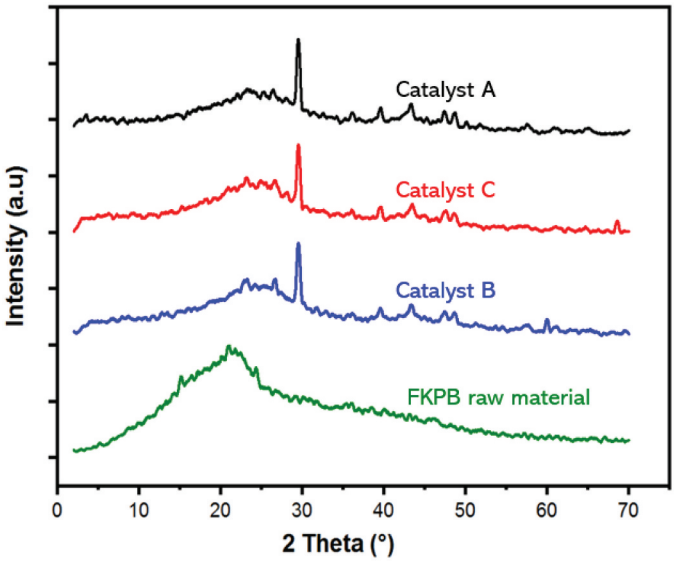

Figure 5. XRD spectra of catalyst A, B and C in comparison to FKPH raw material.

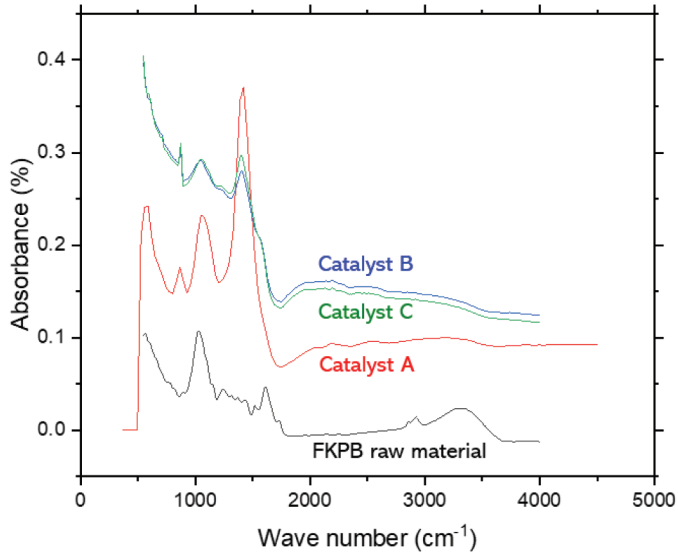

Figure 6. FTIR results of catalyst A, B and C in comparison to FKPH raw material.

absent in the FKPH sample and could be caused by carbohydrate-lignin matrix (Balajii and Niju 2019).

It is apparent that distinct peaks were observed in Catalysts A, B, and C samples between 2 Theta of 2–70° and it can be ascribed to the efficacy of the chosen calcination temperature and treatment by methanol, which has aided the removal of the above-mentioned matrix. In the Catalysts A, B, and C diffractograms, the peaks at 2.99°, 29.58°, 39.56°, 43.39°, 59.92°, and 68.54° can be attributed to the occurrence of minerals tetragonal structured potassium and hexagonal structured calcium that were found to be the key phases of the three formed biocatalysts. Additionally, the minor peak matches elements such as the cubic structured magnesium, which was detected in the Catalysts B and C. After calcination, the mineral magnesium was observed as magnesium oxide (cubic); calcium as calcium oxide (cubic); and potassium as potassium oxide (cubic). From the XRD results, it can be observed that the selected calcination temperature has proven to be effective in the extraction and boost of the minerals in the biocatalysts that is desirable for good catalytic activities (Balajii and Niju 2019).

3.6. FTIR Analysis

The Infra-Red (IR) spectra for the fermented kola nut pod husk FKPH sample and the three catalyst samples are shown in Figure 6. For the FKPH sample, two major absorption peaks were observed at the functional group region. The first peak falls within the 1680–1750 cm^{-1} in the IR Spectroscopy correlation tables region, at exactly 1750 cm^{-1} indicative of the C= O stretching of the carbonyl group present in the fresh sample. The second peak is seen at 3000 cm^{-1}, which lies in the region 2500–3300 cm^{-1} and is allocated to stretching vibrations of O-H group of water molecules (Betiku et al. 2019; Hameed, Lai, and Chin 2009). Comparing the absorption peaks of The Catalyst A and Catalyst C, it was observed that the region between 2500–3300 cm^{-1} disappeared because of the calcination. This indicates the removal of O-H group of water molecules (Betiku et al. 2019; Hameed, Lai, and Chin 2009). However, a major absorption peak was obtained for both calcined samples. This peak was observed at 1750 cm^{-1} which falls in the region of 1680–1750 cm^{-1} indicative of C= O stretching of the carbonyl group (Betiku et al. 2019; Hameed, Lai, and Chin 2009).

In Figure 6, the fact that FKPH and Catalyst A are similarly showing that calcination of the feedstock without treatment with methanol, drying and ash removal has little or no effect on the functional group. However, when the feedstock (FKPH) was treated with methanol and subsequently dried and calcined (Catalyst B), there is an absence of the hydroxyl group in the calcined sample showing the removal of water molecules. In addition, the close resemblance of the spectra of Catalyst B and C implies that there is no significant change in functional group if the ash was removed after calcination. The results obtained in this study was compared with the work of Betiku et al (Betiku et al. 2019), who investigated the functional groups of raw, burnt, and calcined kolanut pods. Slight differences in the functional groups of the feedstock reported in the report of Betiku et al (Betiku et al. 2019) and this study could be attributed to the difference in environmental conditions in which both samples were grown.

4. Conclusions

This present research has explored different treatment methods for the synthesis of green biocatalysts from fermented kola nut pod husk. The catalysts were characterized using SEM-EDS, XRD, XRF, BET, BJH, and FTIR analyses. The characterization results have indicated that the calcination temperature (700°C for 4 h) has had a major impact in drastically extracting and boosting the mineral compositions inherent in the kola nut pod husk by degrading the carbohydrate lignin-matrix. The produced calcined catalysts have shown great catalytic potential due to the high K, Ca, and Mg contents, increased surface area and the existence of mixed mineral oxides such as CaO, MgO, and K_2O. The synthesized catalysts showed an excellent surface area (420–436 m2/g) which is essential property as a catalyst as it

provides sufficient substrate required for the proposed esterification reaction. In addition, the porosity was observed to vary from microporous to macro porous range which is characteristic of hierarchical pore structure which has a wide range of applications including as a catalyst. The results of EDX, FTIR, and XRD indicates that K, Mg, and Ca are the major metals present in Catalysts A, B, and C. This has been shown to have strong catalytic characteristics in biodiesel production. The presence of carbohydrate-lignin matrix was identified in the calcined samples but not in the feedstock which showed the effect of thermal treatment on the samples. In addition, the calcined samples showed more of crystalline nature as observed by the characteristic peak around 30 degrees on the 2Θ axis. These suggest good catalytic properties required for the intended application for biodiesel production.

Acknowledgements

The Author Asuquo Jackson Asuquo would thank the Petroleum Technology Development Fund of Nigeria for sponsoring his PhD study at the University of Strathclyde.

Funding

This work was supported by the Petroleum Technology Development Fund.

References

Abu-Jrai, A. M., F. Jamil, A. H. Al-Muhtaseb, M. Baawain, L. Al-Haj, M. Al-Hinai, M. Al-Abri, and S. Rafiq. 2017, Mar. Valorization of waste date pits biomass for biodiesel production in presence of green carbon catalyst. *Energy Conversion and Management* 135:236–43. doi: 10.1016/j.enconman.2016.12.083.

Adepoju, T. F., M. A. Ibeh, E. O. Babatunde, A. J. Asuquo, and G. S. Abegunde. 2020, Jul. Appraisal of CaO derived from waste fermented-unfermented kola nut pod for fatty acid methylester (FAME) synthesis from Butyrospermum parkii (Shea butter) oil. *South African Journal of Chemical Engineering* 33:160–71. doi: 10.1016/j.sajce.2020.07.008.

Adepoju, T. F., B. E. Olatunbosun, O. M. Olatunji, and M. A. Ibeh. 2018, Dec. Brette Pearl Spar Mable (BPSM): A potential recoverable catalyst as a renewable source of biodiesel from Thevetia peruviana seed oil for the benefit of sustainable development in West Africa. *Energy, Sustainability and Society* 8(1):23. doi: 10.1186/s13705-018-0164-1.

Adepoju, T. F., O. M. Olatunji, M. A. Ibeh, A. S. Kamoru, B. E. Olatunbosun, and A. J. Asuquo. 2020, Jul. Heavea brasiliensis (Rubber seed): An alternative source of renewable energy. *Scientific African* 8:e00339. doi: 10.1016/j.sciaf.2020.e00339.

Adepoju, T. F., B. Rasheed, O. M. Olatunji, M. A. Ibeh, F. T. Ademiluyi, and B. E. Olatunbosun. Sep 2018. Modeling and optimization of lucky nut biodiesel production from lucky nut seed by pearl spar catalysed transesterification. *Heliyon* 4 (9):e00798. doi:10.1016/j.heliyon.2018.e00798.

Adepoju, T. F., E. N. Udoetuk, B. E. Olatunbosun, I. A. Mayen, and R. Babalola. 2018, Jun. Evaluation of the effectiveness of the optimization procedure with methanolysis of waste oil as case study. *South African Journal of Chemical Engineering* 25:169–77. doi: 10.1016/j.sajce.2018.05.002.

Ahmad, J., U. Rashid, F. Patuzzi, M. Baratieri, and Y. H. Taufiq-Yap. 2018, Feb. Synthesis of char-based acidic catalyst for methanolysis of waste cooking oil: An insight into a possible valorization pathway for the solid by-product of gasification. *Energy Conversion and Management* 158:186–92. doi: 10.1016/j.enconman.2017.12.059.

Asogwa, E. U., J. C. Anikwe, and F. C. Mokwunye, 'Kola production and utilization for economic development', 2006. [Online]. http://www.klobex.orgAFS2006034/7410

Balajii, M., and S. Niju. 2019, Jun. A novel biobased heterogeneous catalyst derived from Musa acuminata peduncle for biodiesel production – Process optimization using central composite design. *Energy Conversion and Management* 189:118–31. doi: 10.1016/J.ENCONMAN.2019.03.085.

Baskar, G., and S. Soumiya. 2016. Production of biodiesel from castor oil using iron (II) doped zinc oxide nanocatalyst. *Renew Energy* 98 (Dec):101–07. doi:10.1016/j.renene.2016.02.068.

Betiku, E., A. M. Akintunde, and T. V. Ojumu. 2016. Banana peels as a biobase catalyst for fatty acid methyl esters production using Napoleon's plume (bauhinia monandra) seed oil: A process parameters optimization study. *Energy* 103 (May):797–806. doi:10.1016/J.ENERGY.2016.02.138.

Betiku, E., A. A. Okeleye, N. B. Ishola, A. S. Osunleke, and T. V. Ojumu. 2019. Development of a novel mesoporous biocatalyst derived from kola nut pod husk for conversion of kariya seed oil to methyl esters: A case of synthesis, modeling and optimization studies. *Catalysis Letters* 149 (7):1772–87. doi:10.1007/s10562-019-02788-6.

Bharti, P., B. Singh, and R. K. Dey. 2019, Dec. Process optimization of biodiesel production catalyzed by CaO nanocatalyst using response surface methodology. *Journal of Nanostructure in Chemistry* 9 (4):269–80. doi: 10.1007/s40097-019-00317-w.

Bora, A. P., S. H. Dhawane, K. Anupam, and G. Halder. 2018. Biodiesel synthesis from Mesua ferrea oil using waste shell derived carbon catalyst. *Renew Energy* 121 (Jun):195–204. doi:10.1016/j.renene.2018.01.036.

Chouhan, A. P. S., and A. K. Sarma. 2013, Aug. Biodiesel production from Jatropha curcas L. oil using Lemna perpusilla Torrey ash as heterogeneous catalyst. *Biomass & bioenergy* 55:386–89. doi: 10.1016/j.biombioe.2013.02.009.

Dhawane, S. H., T. Kumar, and G. Halder. 2016. Biodiesel synthesis from Hevea brasiliensis oil employing carbon supported heterogeneous catalyst: Optimization by Taguchi method. *Renew Energy* 89 (Apr):506–14. doi:10.1016/j.renene.2015.12.027.

Etim, A. O., A. C. Eloka-Eboka, and P. Musonge. 2020, Sep. Potential of Carica papaya peels as effective biocatalyst in the optimized parametric transesterification of used vegetable oil. *Environmental Engineering Research* 26(4):200299–0. doi: 10.4491/eer.2020.299.

Etim, A. O., A. C. Eloka-Eboka, and P. Musonge. 2021, Aug. Potential of carica papaya peels as effective biocatalyst in the optimized parametric transesterification of used vegetable oil. *Environmental Engineering Research* 26(4):200299–0. doi: 10.4491/eer.2020.299.

European Climate Foundation, 'The European green deal', *European Climate Foundation*, 2023. https://europeanclimate.org/the-european-green-deal/ (accessed Oct. 27, 2022).

Falowo, O. A., and E. Betiku. 2022. A novel heterogeneous catalyst synthesis from agrowastes mixture and application in transesterification of yellow oleander-rubber oil: Optimization by Taguchi approach. *Fuel* 312 (Mar):122999. doi:10.1016/J.FUEL.2021.122999.

Falowo, O. A., T. V. Ojumu, O. Pereao, and E. Betiku. 2020, Feb. Sustainable biodiesel synthesis from honne-rubber-neem oil blend with a novel mesoporous base catalyst synthesized from a mixture of three agrowastes. *Catalysts* 10(2):190. doi: 10.3390/catal10020190.

Gohain, M., A. Devi, and D. Deka. 2017. Musa balbisiana Colla peel as highly effective renewable heterogeneous base catalyst for biodiesel production. *Industrial Crops & Products* 109 (Dec):8–18. doi:10.1016/J.INDCROP.2017.08.006.

Hameed, B. H., L. F. Lai, and L. H. Chin. Apr 2009. Production of biodiesel from palm oil (elaeis guineensis) using heterogeneous catalyst: An optimized process. *Fuel Processing Technology* 90 (4):606–10. doi:10.1016/j.fuproc.2008.12.014.

Kamble, A. D., V. A. Mendhe, P. D. Chavan, and V. K. Saxena. 2022. Insights of mineral catalytic effects of high ash coal on carbon conversion in fluidized bed Co-gasification through FTIR, XRD, XRF and FE-SEM. *Renew Energy* 183 (Jan):729–51. doi:10.1016/J.RENENE.2021.11.022.

Kostić, M. D., A. Bazargan, O. S. Stamenković, V. B. Veljković, and G. McKay. 2016. Optimization and kinetics of sunflower oil

methanolysis catalyzed by calcium oxide-based catalyst derived from palm kernel shell biochar. *Fuel* 163 (Jan):304–13. doi:10.1016/J.FUEL.2015.09.042.

Lee, H. V., J. C. Juan, N. F. Binti Abdullah, R. Nizah MF, and Y. H. Taufiq-Yap. Dec 2014. Heterogeneous base catalysts for edible palm and non-edible Jatropha-based biodiesel production. *Chemistry Central Journal* 8 (1):30. doi:10.1186/1752-153X-8-30.

Maroa, S., and F. Inambao. Dec 2021. A review of sustainable biodiesel production using biomass derived heterogeneous catalysts. *Engineering in Life Sciences* 21 (12):790–824. doi:10.1002/elsc.202100025.

Mendonça, I. M., O. A. R. L. Paes, P. J. S. Maia, M. P. Souza, R. A. Almeida, C. C. Silva, S. Duvoisin, and F. A. de Freitas. 2019, Jan. New heterogeneous catalyst for biodiesel production from waste tucumã peels (astrocaryum aculeatum Meyer): Parameters optimization study. *Renew Energy* 130:103–10. doi: 10.1016/j.renene.2018.06.059.

Mierczynski, P., R. Ciesielski, A. Kedziora, W. Maniukiewicz, O. Shtyka, J. Kubicki, J. Albinska, and T. P. Maniecki. 2015, May. Biodiesel production on MgO, CaO, SrO and BaO oxides supported on (SrO)(al2o3) mixed oxide. *Catalysis Letters* 145(5):1196–205. doi: 10.1007/s10562-015-1503-x.

Olatundun, E. A., O. O. Borokini, and E. Betiku. 2020. Cocoa pod husk-plantain peel blend as a novel green heterogeneous catalyst for renewable and sustainable honne oil biodiesel synthesis: A case of biowastes-to-wealth. *Renew Energy* 166 (Apr):163–75. doi:10.1016/J.RENENE.2020.11.131.

Olugbenga, A. G., A. Mohammed, and O. N. Ajakaye. 2013. Biodiesel production in Nigeria using cocoa pod ash as a catalyst base. *International Journal of Science & Engineering Investigations* 2:15. [Online]. www.IJSEI.com

Osakwe, E. U., I. J. Ani, U. G. Akpan, and M. A. Olutoye. 2018, Jul. Kolanut pod husk as a biobase catalyst for fatty acid methyl ester production using thevetia peruviana (yellow oleander) seed oil. *IOP Conference Series: Earth and Environmental Science* 173(1):012008. doi: 10.1088/1755-1315/173/1/012008.

Sharma, M., A. A. Khan, S. K. Puri, and D. K. Tuli. 2012, Jun. Wood ash as a potential heterogeneous catalyst for biodiesel synthesis. *Biomass and Bioenergy* 41:94–106. doi: 10.1016/j.biombioe.2012.02.017.

Stanford University, 'Covid lockdown causes record drop in carbon emissions for 2020.' *Stanford Earth Magazine*, Oct. 2020. https://earth.stanford.edu/news/covid-lockdown-causes-record-drop-carbon-emissions-2020#gs.hco7dy. (Accessed Oct. 20, 2021).

Tan, Y. H., M. O. Abdullah, C. Nolasco-Hipolito, and Y. H. Taufiq-Yap. 2015, Dec. Waste ostrich- and chicken-eggshells as heterogeneous base catalyst for biodiesel production from used cooking oil: Catalyst characterization and biodiesel yield performance. *Applied Energy* 160:58–70. doi: 10.1016/J.APENERGY.2015.09.023.

Tan, D., Y. Wu, L. Junshuai, L. Jian, O. Xiaoyu, Y. Meng, G. Lan, Y. Chen, and Z. Zhang. 2023. 'Performance optimization of a diesel engine fueled with hydrogen/biodiesel with water addition based on the response surface methodology. *Energy* 263 (part C):125869. doi:10.1016/j.energy.2022.125869.

Thommes, M., K. Kaneko, A. V. Neimark, J. P. Olivier, F. Rodriguez-Reinoso, J. Rouquerol, and K. S. W. Sing. 2015, Oct. Physisorption of gases, with special reference to the evaluation of surface area and pore size distribution (IUPAC technical report). *Pure and Applied Chemistry* 87(9–10):1051–69. doi: 10.1515/pac-2014-1117.

Uddin, M. R., K. Ferdous, M. R. Uddin, M. R. Khan, and M. A. Islam. 2013, Apr. Synthesis of biodiesel from waste cooking oil. *Chemical Engineering and Science* 1(2):22–26. doi: 10.12691/ces-1-2-2.

UN, 'World kola nut production', *UN Data Statistics*, Jun. 22, 2022. http://data.un.org/Data.aspx?d=FAO&f=itemCode%3A224 (accessed Feb. 20, 2023).

Vadery, V., B. N. Narayanan, R. M. Ramakrishnan, S. K. Cherikkallinmel, S. Sugunan, D. P. Narayanan, and S. Sasidharan. 2014, Jun. Room temperature production of jatropha biodiesel over coconut husk ash. *Energy* 70:588–94. doi: 10.1016/j.energy.2014.04.045.

Zhao, C., P. Lv, L. Yang, S. Xing, W. Luo, and Z. Wang. 2018, Mar. Biodiesel synthesis over biochar-based catalyst from biomass waste pomelo peel. *Energy Conversion and Management* 160:477–85. doi: 10.1016/j.enconman.2018.01.059.